Coherent Versus Noncoherent Signaling for Satellite-Aided Mobile Communications

F. Davarian
J. Sumida

October 15, 1986

NASA

National Aeronautics and
Space Administration

Jet Propulsion Laboratory
California Institute of Technology
Pasadena, California

Coherent Versus Noncoherent Signaling for Satellite-Aided Mobile Communications

F. Davarian
J. Sumida

October 15, 1986

NASA

National Aeronautics and
Space Administration

Jet Propulsion Laboratory
California Institute of Technology
Pasadena, California

ABSTRACT

The use of coherent versus noncoherent communications is an unresolved issue
for the mobile satellite community. Should one select the more robust but
less efficient noncoherent strategy for communications over satellite-aided
mobile channels, or does the introduction of a space platform in the mobile
link improve signal stability (both amplitude and phase) such that
conventional coherent schemes become attractive? This publication tries to
answer some of the questions by discussing the results from experiments using
a coherent QPSK receiver.

The issues discussed in this publication include items such as the measured
performance in Rician fading, the link error floor in a fading environment,
etc. The results are compared and contrasted with that of a noncoherent
limiter/discriminator FM receiver.

CONTENTS

<u>Figures</u>

CONTENTS (Contd)

Tables

I. INTRODUCTION

The performance and behavior of narrowband coherent and noncoherent digital receivers in a terrestrial mobile communications environment have been documented in the literature [1,2]. The fading phenomenon associated with a terrestrial mobile system is generally modeled as a Rayleigh distribution. Furthermore, the simplicity of the Rayleigh model permits performance prediction by analytical tools [3]. Because of the infancy of mobile communications by satellite, very little is published on the performance of different receiver types in such channels. The objective of this publication is to report on the recent experiments conducted to examine the behavior of a coherent QPSK receiver in a mobile satellite environment. The main issues addressed are error performance in thermal noise and fading, link error floor, frequency offset, and spectrum occupancy. The statistics of satellite-aided mobile communications are widely modeled by a more complicated distribution known as Rician [4]. The Rician model used in this publication assumes a specular to diffused ratio of 10 dB.

For the purpose of comparison, the experiments presented in this publication are compared to similar experiments using a noncoherent receiver for detection of a 2400-bps minimum shift keying (MSK) signal. This noncoherent receiver consists of a frequency discriminator and is described in [5].

II. THE MODULATOR

Signal modulation is performed by the Multipurpose All-Digital Transmitter (MADT). The architecture of this transmitter is described in [6]. Employing an elaborate technique, this transmitter generates a near ideal QPSK signal which is pulse shaped using a raised-cosine, pulse-shaping filter with an excess bandwidth of 100 percent. For simplicity, the full filter is realized in the transmitter rather than equally sharing the filter in the two ends of the link. The resulting signal spectrum is shown in Figure 1 for a 2400-bps source. Figure 2 shows the eye diagram of the signal at the transmitter. This eye diagram is relatively free from distortion.

|←————————5 kHz————————→|
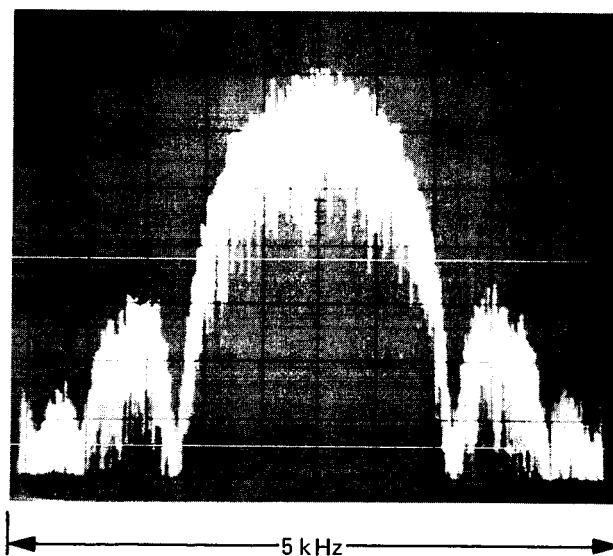
VERTICAL SCALE: 10 dB per division

Figure 1. Transmitted Signal Spectrum
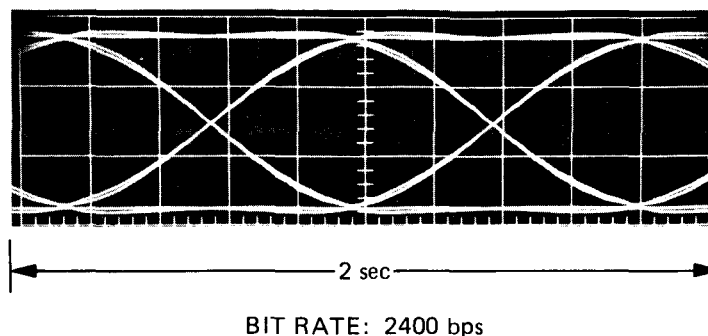
1

2 sec

BIT RATE: 2400 bps

Figure 2. Data Eye Diagram at the Transmitter

To assist the Costas receiver in resolving the four-fold phase ambiguity of the carrier, data are differentially encoded before modulating the carrier. The differential codec is described in Appendix A.

III. THE RECEIVER

The receiver is a conventional Costas-loop coherent receiver. Since the full pulse-shaping filter was realized at the transmitter, the receiver filter is approximated by a brick-wall filter. Because of this simplification, i.e., full filter implementation at the transmit end, the receiver performance suffers by 3 dB. In the experimental results reported in this publication, the above 3-dB loss is ignored. Figure 3 shows the receiver block diagram. This receiver includes the Costas loop, AGC loop, two brick-wall filters, two sample-and-hold circuits, and the differential decoder. The input frequency is 50 MHz. The bit timing is delivered from the transmitter by hard wiring; hence, the experiments reported below do not contain the bit-sync-induced distortions. Such distortions, however, are envisioned to be small. A slight performance loss due to differential data encoding is associated with this receiver. The specific hardware parameters of the receiver are given in Appendix B.
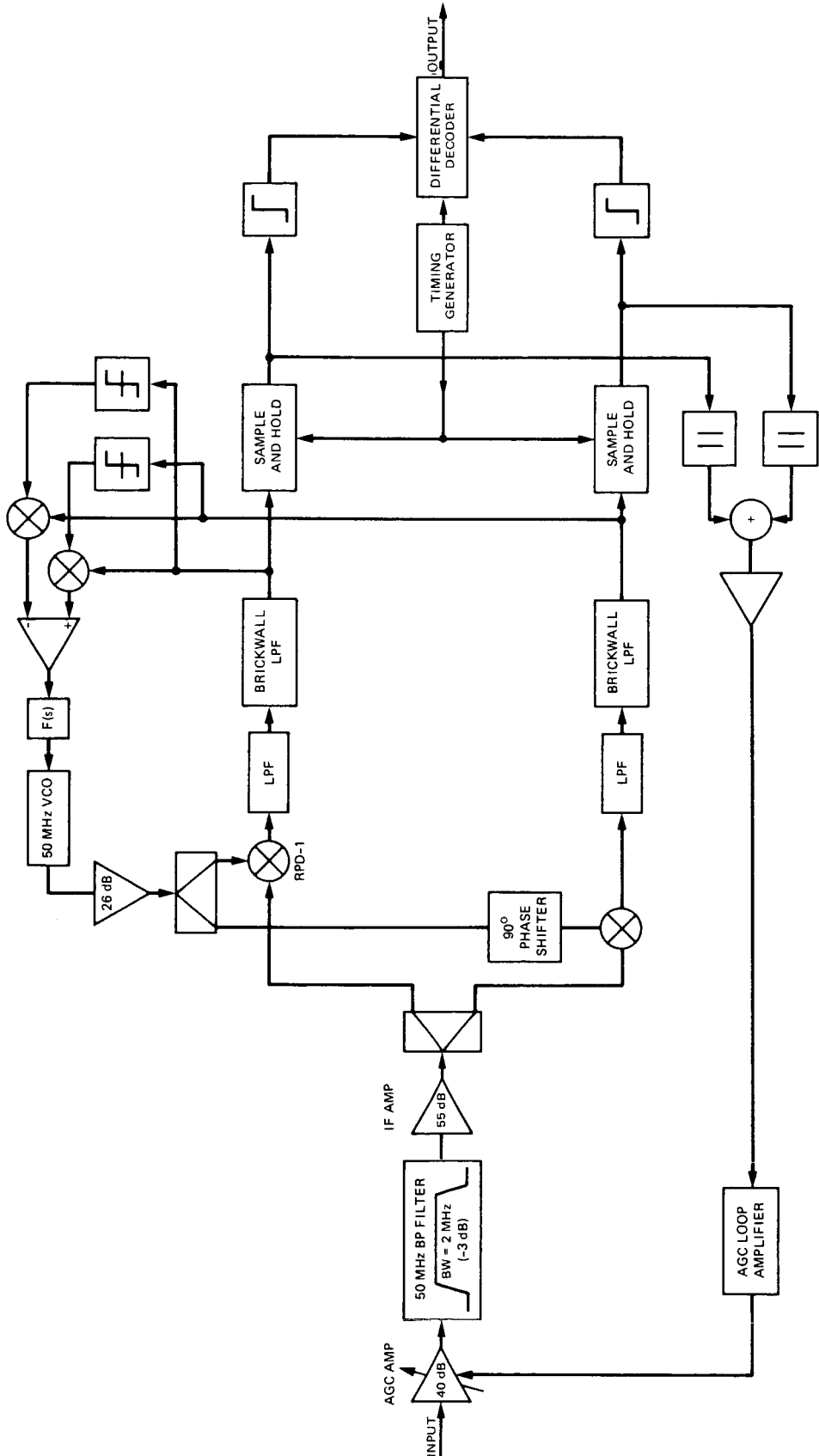
Figure 3. Receiver Block Diagram

IV. THE EXPERIMENTS

The experiments described herein were conducted at the mobile satellite channel simulator. This channel simulator is described in [4]. The transmitted data were generated by a PN data generator at a rate of 2400 bps. The 50-MHz, QPSK-modulated carrier is sent through the channel simulator and then received and demodulated by the receiver; the detected bits are compared to the transmitted ones for bit-error-rate measurement.

Figure 4 demonstrates the measured bit error rate as a function of the E_b/N_o ratio in a purely Gaussian channel. The measured performance is about 0.6 dB poorer than ideal BPSK performance. Part of this loss is due to hardware and part is due to differential encoding of data. For comparison, a similar curve for a noncoherent MSK receiver is shown on the same figure. At a bit error rate of 0.001, the coherent receiver is about 3.5 dB better than the noncoherent one.

Figure 4. Measured Bit Error Rate in the Presence of Thermal Noise

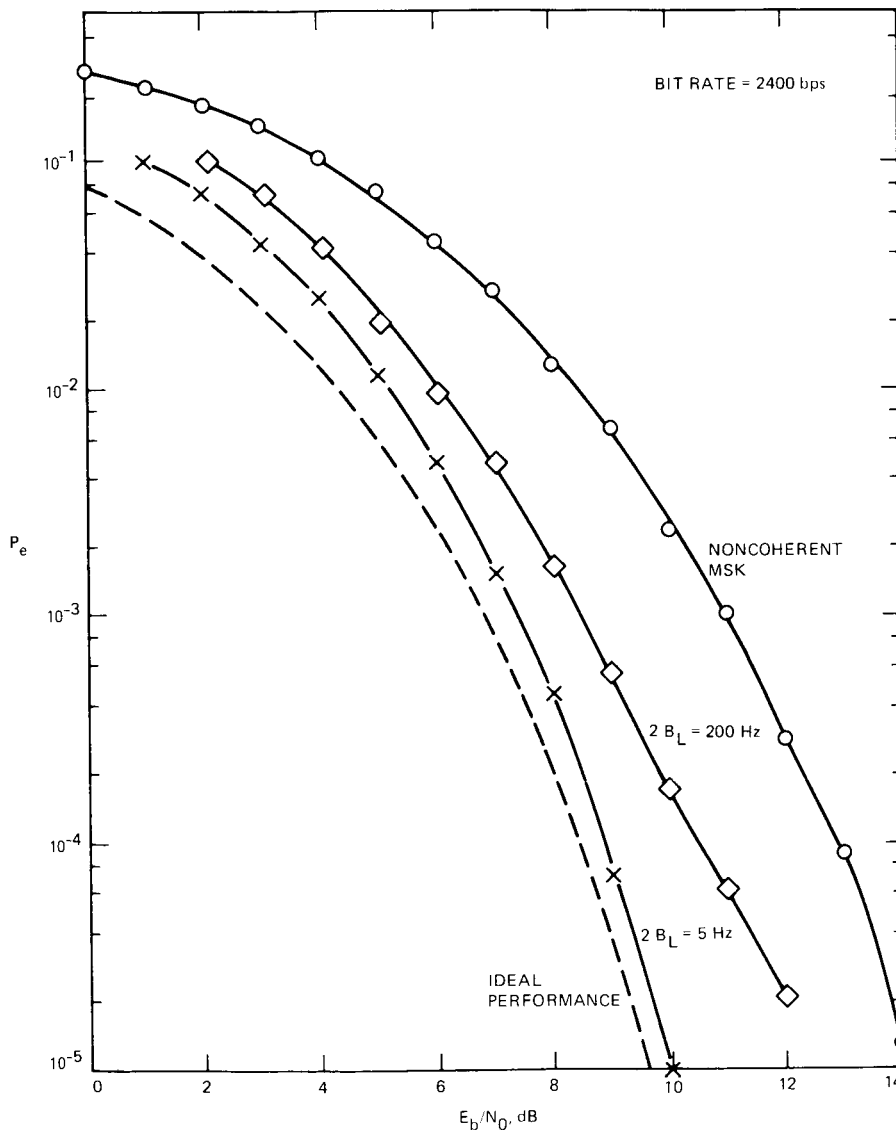To optimize the measurements shown in Figure 4, the receiver's carrier-tracking loop bandwidth (double-sided) was set very low, at 5 Hz. Since such a narrowband loop is not suitable for the reception of fading signals, a similar experiment was conducted with the loop bandwidth set at 200 Hz. The result of this experiment is also shown in Figure 4. Comparing the two results reveals that a loss of about 1 dB is incurred because of an increase in the loop bandwidth, at a bit error rate of 0.001. For lower bit error rates, this loss is even greater.

To examine the receiver behavior in the presence of a frequency offset, Figure 5 is presented. This figure shows that a frequency offset of 100 Hz results in a modest power loss of about 0.3 dB. Again for the purpose of comparison, it is noted in [5] that an MSK noncoherent receiver suffers from a loss of about 1 dB for a frequency offset of 100 Hz. Hence, the coherent receiver is superior to a noncoherent receiver in channels impaired by thermal noise and frequency error.
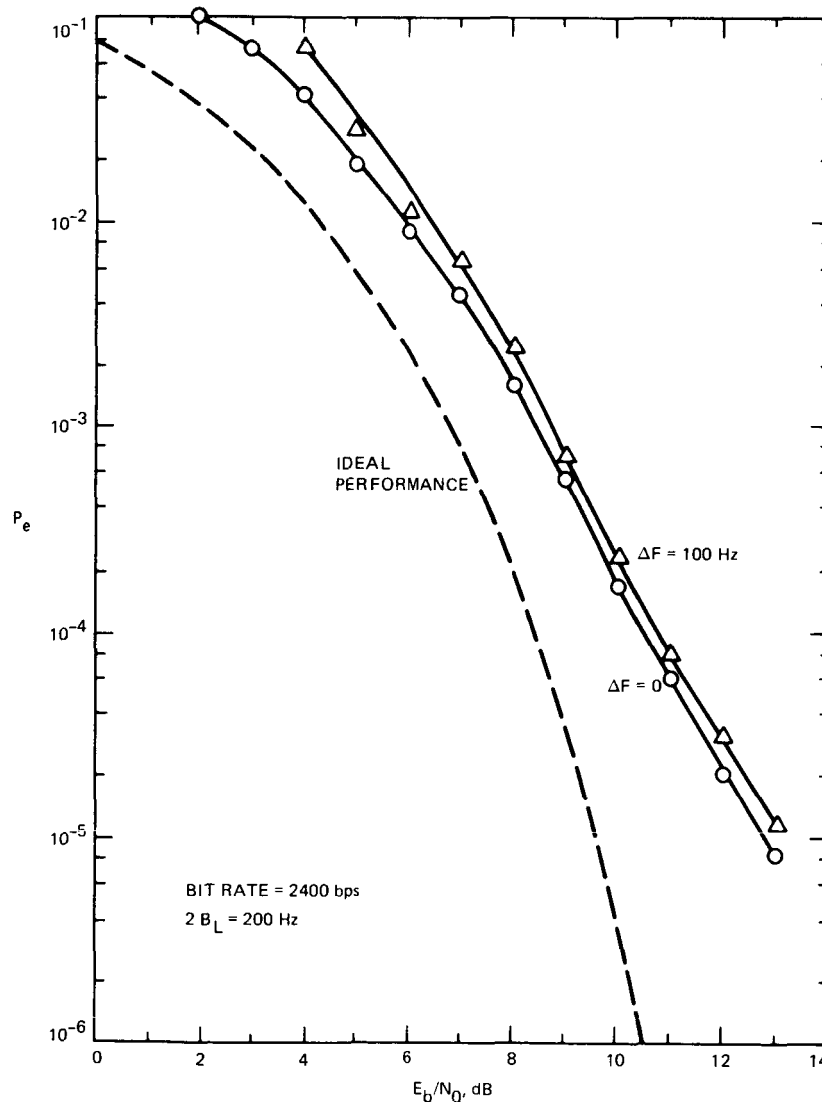

Figure 5.   Receiver Error Performance in the Presence of a Frequency Offset of 100 Hz

The receiver performance in the presence of Rayleigh fading is shown in Figure 6. The Rayleigh-fading behavior is clearly plagued by a very high error floor even for a relatively small Doppler of 20 Hz. The curves illustrating the Rician fading situation are presented in Figure 7. The curves show substantial improvement with respect to the Rayleigh case. For comparison a similar curve for the noncoherent receiver is also shown in this figure. Although the noncoherent performance is better (since it suffers from a lower error floor), the E_b/N_o, which results in an error rate of 0.001, is about 14 dB for both receivers.

To explore the impact of the carrier-tracking loop bandwidth on the link error floor, Figure 8 is presented. This figure shows the link error floor as a function of the two-sided loop bandwidth. It appears that the best performance for both Rayleigh and Rician channels is achieved around a bandwidth of 200 Hz.
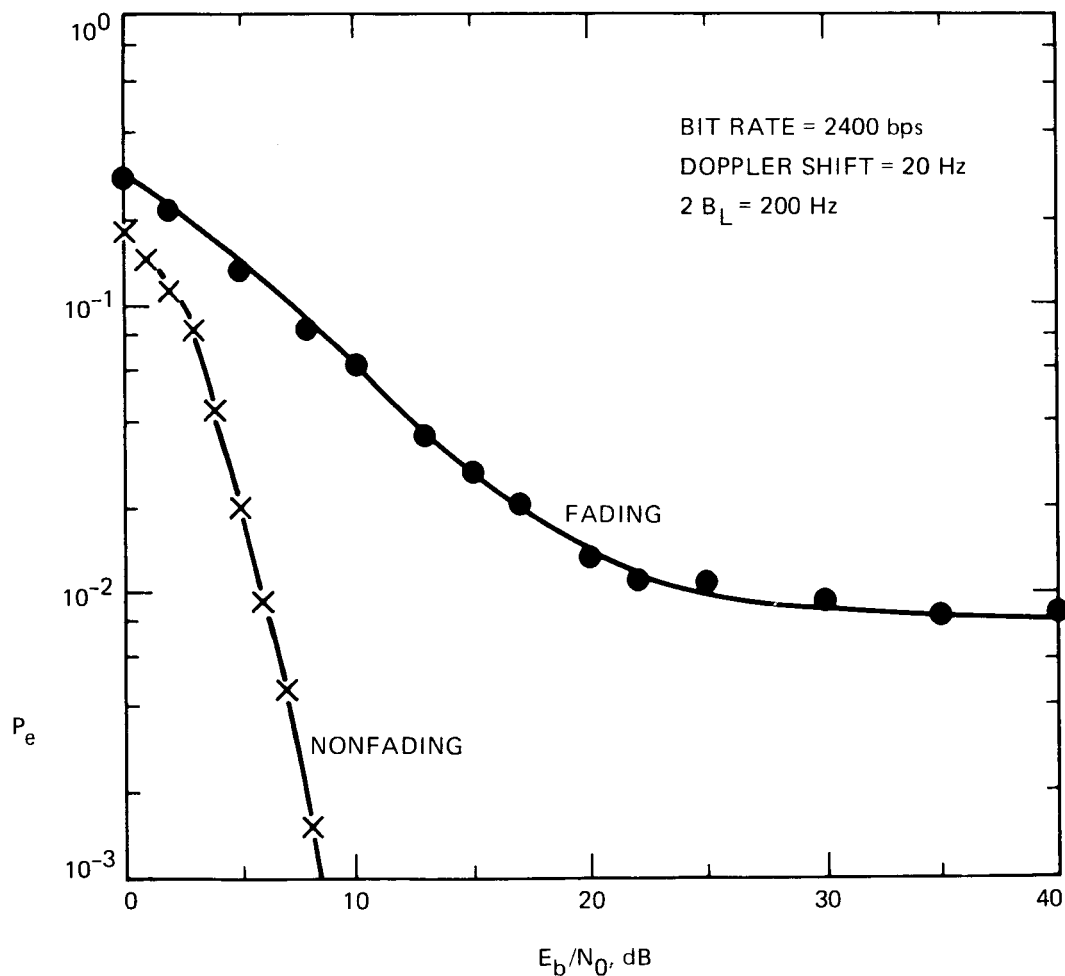
Figure 6. Measured Error Performance in the Presence of Rayleigh Fading
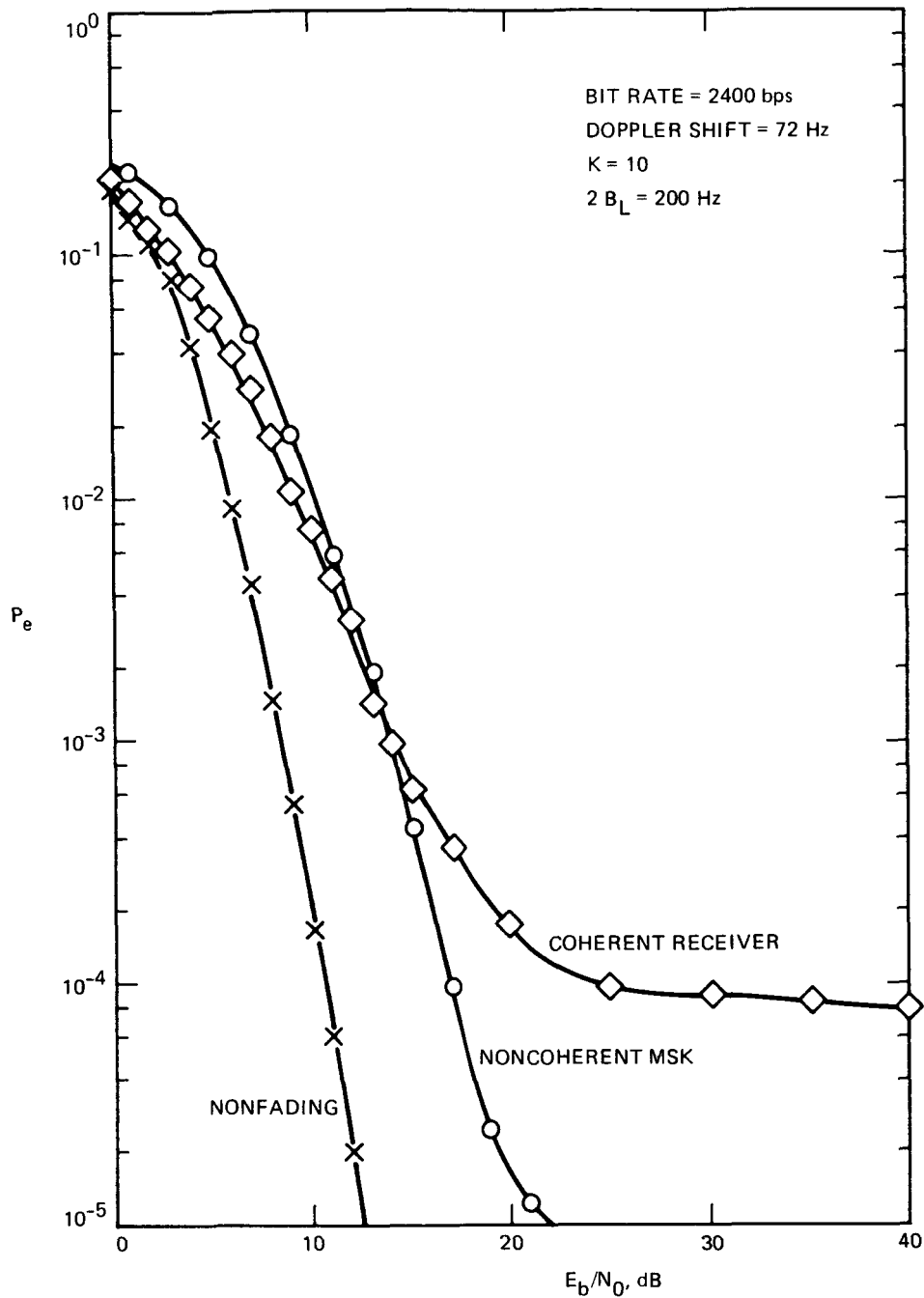
Figure 7. Measured Error Performance in the Presence of Rician Fading

Before observing the result of Figure 8, it had been assumed that the error floor is a monotonically decreasing function of the loop bandwidth. This assumption would have been correct if the QPSK signal was not filtered. Note that the Nyquist filtering of data results in a nonconstant envelope signal, which affects the carrier-tracking loop performance. For small values of the loop bandwidth, the effect of signal amplitude variations on the locally generated carrier is small. As the loop bandwidth is increased, the locally generated carrier phase becomes strongly influenced by the signal amplitude.

7

Using a storage oscilloscope, attempts were made to measure the acquisition time of the receiver in the presence of 100 Hz of frequency offset (or Doppler) when E_b/N_o = 10 dB and the carrier-tracking loop bandwidth (double-sided) is 200 Hz. The test showed rather a nonstationary behavior in the sense that for the majority of trials the acquisition was achieved in less than 20 ms (44 bits), but in a few instances the acquisition took longer than 50 ms (120 bits). It should be mentioned that the receiver tested had not been designed to minimize acquisition time.
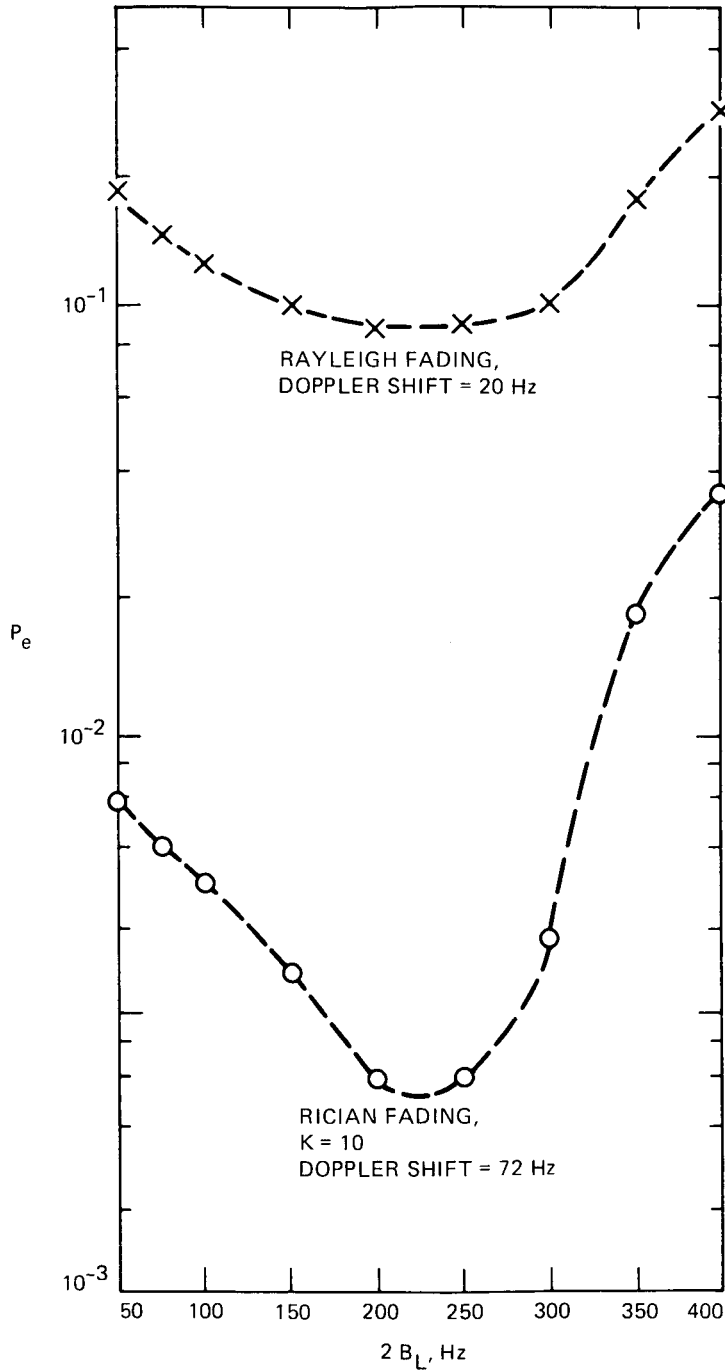

Figure 8. Observed Error Floor as a Function of Two-Sided Loop Bandwidth

V. CONCLUSION

The performance of a 2400-bps coherent QPSK receiver in simulated satellite-aided mobile channels was experimentally determined. The results were compared to that of a noncoherent MSK receiver. It was shown that the steady-state performance of the coherent receiver, when the channel is impaired only by thermal noise and frequency offset, is substantially superior to that of a noncoherent receiver. For a Rayleigh fading signal, however, a noncoherent receiver is substantially better. In the case of Rician fading, i.e., a mobile satellite channel, a noncoherent receiver slightly overperforms the coherent system with a specular to diffuse ratio of 10 dB. In conclusion, it may be said that for fading channels with a specular to diffuse ratio of 10 dB or lower a noncoherent scheme is preferable, whereas when this ratio is higher than 10 dB, the coherent technique is more advantageous. For cases where a short acquisition time is of prime concern, a noncoherent approach is always preferable.

REFERENCES

1. S. Good, "A Comparison of Gaussian Minimum Shift Keying to Frequency Shift Keying for Land Mobile Radio," 34th IEEE Vehicular Conference, Pittsburgh, PA, May 1984.

2. G. Arredondo, et al., "Voice and Data Transmission," Bell System Technical Journal (special issue on Advanced Mobile Phone Service), Vol. 58, No. 1, Jan. 1979.

3. W. Lee, Mobile Communications Engineering, pp. 403-404, McGraw-Hill, 1982.

4. F. Davarian, "Channel Simulation to Facilitate Mobile-Satellite Communications Research," IEEE Trans. Communications, Vol. Com-34, No. 12, Dec. 1986.

5. A. Densmore, "Evaluation of a Narrowband Noncoherent FM Receiver," JPL internal memo, Oct. 1986.

6. F. Davarian and J. Sumida, "A Multipurpose All-Digital Transmitter," IEEE MONTECH Conference, Sept. 1986.

DIFFERENTIAL DATA ENCODING TO RESOLVE PHASE AMBIGUITIES
OF A COHERENT QPSK RECEIVER

I. Introduction

Coherent demodulation of a data-bearing carrier is hindered by the potential phase ambiguity of the carrier-regeneration circuit of the receiver. Conventional carrier tracking systems, such as the well known Costas loop, suffer from an N-fold phase ambiguity, where N is an integer denoting the number of phase divisions of the carrier. Differential encoding of the data at the transmitter can assist the receiver in neutralizing this potential phase uncertainty. Weber [1] has addressed the differential encoding issue in general for multiple amplitude and phase shift keying systems. This appendix focuses on a subset of the data modulation schemes considered in [1] known as quadrature phase shift keying (QPSK). The main advantage of the technique described in this appendix lies in its simplicity. Both the encoder and the decoder are implemented by very simple logic circuits. Note that QPSK is perhaps the most widely used digital signaling scheme today. In addition to the correct phase, the QPSK receiver can lock on three more points, offset by $\pi/2$, π, or $3\pi/2$.

In a QPSK transmitter, the binary source output is sampled two bits at a time with the first bit transmitted over the in-phase channel and the second transmitted over the quadrature channel. The process of differential encoding requires, before transmission, conversion of each pair of bits into a new pair, according to some encoding rule. The receiver, on the other hand, will pair back together the received bits of the in-phase and quadrature channels and, according to some decoding rule, will make a decision as to which pair of bits (or symbol) was transmitted. The objective of this appendix is to present a simple encoding/decoding rule that will automatically eliminate the problem of carrier phase ambiguity at a QPSK receiver.

II. The Coding Scheme

The carrier phase plane consists of four quadrants, and the four phase positions can be denoted by pairs of data points on the in-phase and quadrature channels or axes. The phase position in the first quadrant can be addressed by (1,1) and the other three phases can, respectively, be addressed by (0,1), (0,0), and (1,0), as shown in Figure A-1. Note that in these coordinates, the first bit denotes the data polarity on the in-phase channel, and the second bit denotes the data polarity on the quadrature channel (this order can also be reversed).
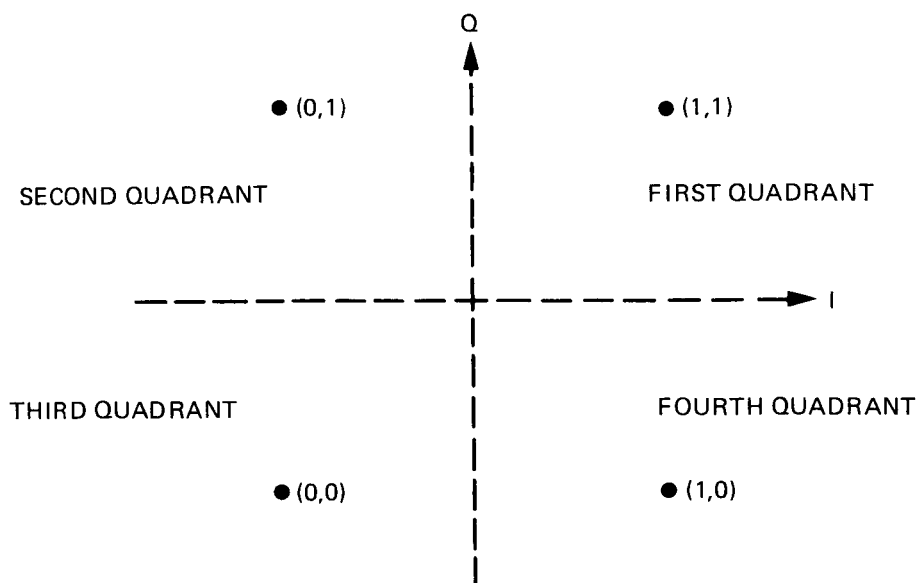
Figure A-1. Transmitter Signal Constellation

We may arbitrarily use the following pairs of bits to denote the potential phase changes that may occur in a QPSK system.

Table A-1. Potential Phase Changes in a QPSK System

Position	Change
(1,1)	0
(0,1)	$\frac{\pi}{2}$
(1,0)	$\frac{-\pi}{2}$
(0,0)	π

Thus, rather than encoding the source output into an absolute phase, we may use the relationships of Table A-1 to differentially encode the source output. Hence, each new bit pair of the source output will determine if the carrier phase is advanced or retarded by some multiple of $\pi/2$.

Example: Assuming the initial phase position is at (1,1), i.e., the first quadrant, determine the transmitted in-phase and quadrature data if the source output is given by "10001011".

Solution: We will first break up the source output into pairs as (1,0), (0,0), (1,0), (1,1). This implies, according to Table A-1, phase transitions of $-\pi/2$, π, $-\pi/2$, and 0. Hence, starting from the first quadrant, the following sequence will occur: 4,2,1,1. In terms of the addresses on the in-phase and quadrature channels, the data pairs corresponding to the above sequence are (1,0), (0,1), (1,1), and (1,1). Hence, the bits in the first location of the above address sequence determine the in-phase signal "1011"; likewise, the second set of bits forms the quadrature data as "0111".

The demodulator will utilize the pairs of data from in-phase and quadrature channels to make a decision. These pairs depend on the phase ambiguity of the carrier and are tabulated below.

Phase ambiguity	Data pairs
0	(1,0), (0,1), (1,1), (1,1)
$\frac{\pi}{2}$	(1,1), (0,0), (0,1), (0,1)
$\frac{-\pi}{2}$	(0,0), (1,1), (1,0), (1,0)
π	(0,1), (1,0), (0,0), (0,0)

In terms of quadrants, the above can be represented as follows.

Phase ambiguity	Data positions
0	4, 2, 1, 1
$\frac{\pi}{2}$	1, 3, 2, 2
$\frac{-\pi}{2}$	3, 1, 4, 4
π	2, 4, 3, 3

Now differential decoding of all the above phase sequences yields the following unique sequence: π, $-\pi/2$, 0. The use of Table A-1 results in the final decoded bit stream of "001011". This bit sequence is identical to the last 6 bits of the transmitted bit stream. Therefore, we have demonstrated that the decoded data are independent of the carrier phase ambiguity.

The encoding procedure can be simplified if modulo 4 arithmetic is used. Let the four quadrants be numbered 0, 1, 2, and 3, respectively, in the ascending fashion. The binary source output is grouped in pairs of bits and, by use of Table A-1, each pair is converted into an integer (0, 1, 2, or 3). The resulting numbers are summed in an accumulator using modulo 4 arithmetic. The result is the quadrant to be transmitted. Hence, the output of the quaternary accumulator is encoded "11", "01", "00", and "10" for 0, 1, 2, and 3, respectively, as evident from Figure A-1. Figure A-2 is the block diagram of the encoder.

SINGLE BITS — PAIRS OF BITS — INTEGER 0, 1, 2, OR 3

BINARY SOURCE → SERIAL TO PARALLEL → MAPPER AND MOD 4 SUMMER → BINARY ENCODER

BINARY ENCODER
0 → "11"
1 → "01"
2 → "00"
3 → "10"

TO QPSK MODULATOR
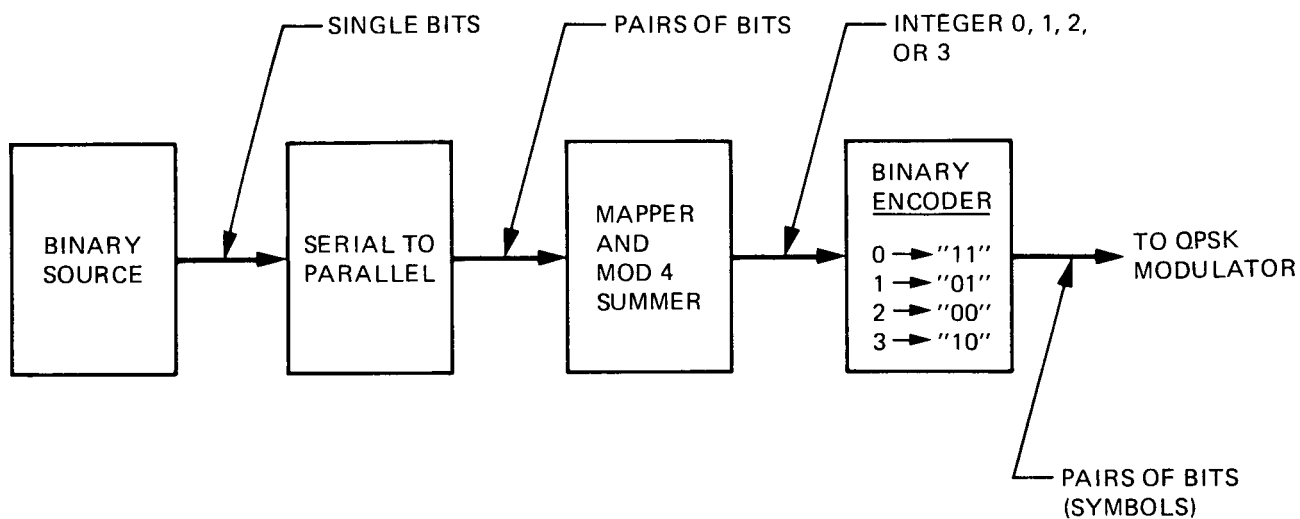
PAIRS OF BITS (SYMBOLS)

Figure A-2. Encoder Block Diagram

The logic representation of Table A-1 is simple. Figure A-3 shows the mapper and mod 4 summer of Figure A-2. Let the input to the mapper be denoted by bits $a_1 a_2$ and the output bits be denoted by $b_1 b_2$. The input/output relationship of the mapper, by use of Table A-1, can be given by the following two logic equations:

$$b_1 = \overline{a_2}$$
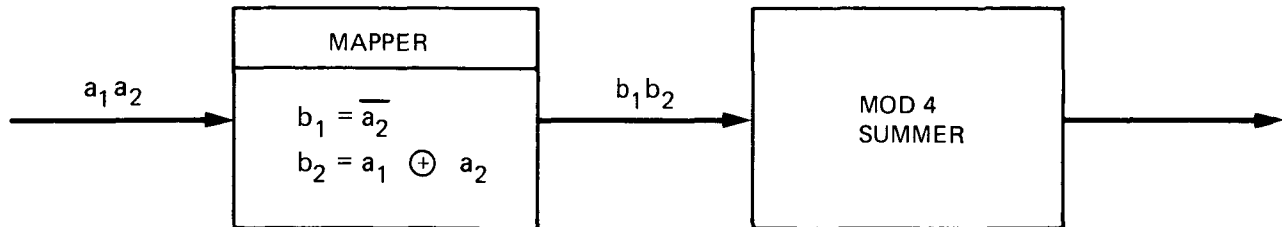$$b_2 = a_1 \oplus a_2 \tag{1}$$

Figure A-3. Mapper and Mod 4 Summer Block Diagram

Note that the mod 4 summer treats the input bits b_1b_2 as a binary number. The summer can be implemented by a two-bit accumulator. The binary encoder of Figure A-2 is realized by the following equations:

$$b_1 = \overline{a_1 \oplus a_2}$$

$$b_2 = \overline{a_1}$$

(2)

where, again, a_1a_2 denotes the input and b_1b_2 denotes the output of the binary encoder.

The receiver observes the pairs of received data and decides which quadrant they correspond to. If the difference between the two consecutively received quadrants is converted into a pair of binary digits (Table A-1), two bits of decoded data will result. The decoder function can be described by the truth table given in Table A-2, where a_1a_2 and b_1b_2 denote two consecutive pairs of bits with index "1" referring to the in-phase channel and "2" referring to the quadrature channel.

Table A-2. Decoder Truth Table

True Logic	Phase	Pair of bits
$(a_1 \oplus a_2)(b_1 \oplus b_2)$	π	(00)
$\overline{(a_1 \oplus a_2)}\,\overline{(b_1 \oplus b_2)}$	0	(11)
$(a_1 \oplus b_2)\overline{(b_1 \oplus a_2)}$	$\dfrac{-\pi}{2}$	(10)
$\overline{(a_1 \oplus b_2)}(b_1 \oplus a_2)$	$\dfrac{\pi}{2}$	(01)

III. The Encoder Performance

Table A-1 is intentionally configured to minimize the link-bit-error probability. A single bit error at the receiver will result in double errors at the output of the decoder. No more than two decoder bit errors can result from a single received error. However, note that double errors at the receiver could cause quadruple errors at the output of the decoder. To demonstrate this, we again use the above example. Supposing no phase ambiguity exists, we assume that the received sequence of paired bits is given by

$$(1,0), \ (0,1), \ (0,0), \ (1,1)$$

Note that in this example the third received pair (symbol) is detected in error. Furthermore, it is evident that this error is caused by two bit errors. The differential decoder will determine the quadrants as 4, 2, 3, 1. The differences between these quadrants are π, $\pi/2$, and π. Hence, using Table A-1, we determine the decoded bits as "000100". The last four bits are different than the ones transmitted.

The effect of differential encoding is to double the bit-error probability at high signal-to-noise ratios (SNR). At low SNR, however, this increase in the bit-error probability is less than double.

Reference

1. W. Weber, "Differential Encoding for Multiple Amplitude and Phase Shift Keying Systems," _IEEE Trans. Communications_, Vol. Com-26, No. 3, March 1978.

APPENDIX B

COSTAS LOOP PARAMETERS AND BRICK-WALL FILTER CHARACTERISTICS

This appendix presents the Costas-loop parameters and the characteristics of the brick-wall filter. The Costas loop is of second-order type with a two-sided bandwidth of 200 Hz; the brick-wall filter bandwidth is 1200 Hz.

Costas Loop Design

Fh = ± 1,200.00 Hz   Hold-in Range
Fp = ±319.14 Hz   Pull-in Range
Go = 7.54E+03 1/sec   Dc Loop Gain
Fo = ±120.00 Hz   Frequency Offset
Spe = 0.100 rad (5.73 deg)   Static Phase Error
2BLo = 200.00 Hz   2 Sided Loop Noise Bandwidth
KVCO = 1.00E+02 Hz/V   VCO Gain
Kd = 0.159 V/rad   Phase-detector Gain Factor
Wn = 188.57 rad/sec   Loop Naturnal Frequency
Tp = 6.00E-02 sec   Pull-in Time
Ka = 75.47   Required Minimum Amplifier Gain
Zeta = 0.707   Damping Factor
T1 = 2.12E-01 sec   Time Constant of Loop Filter
T2 = 7.50E-03 sec   Time Constant of Loop Filter
C = 1.40 mfd   Filter Capacitor
R1 = 1.94 Kohms (2K)   Filter Input Resistor
R2 = 5.36 Kohms (5.6K)   Filter Feedback Resistor
R3 = 146.10 Kohms (150K)   Filter Gain Resistor
Ro = 146.10 Kohms (150K)   Amplifier Offset Resistor
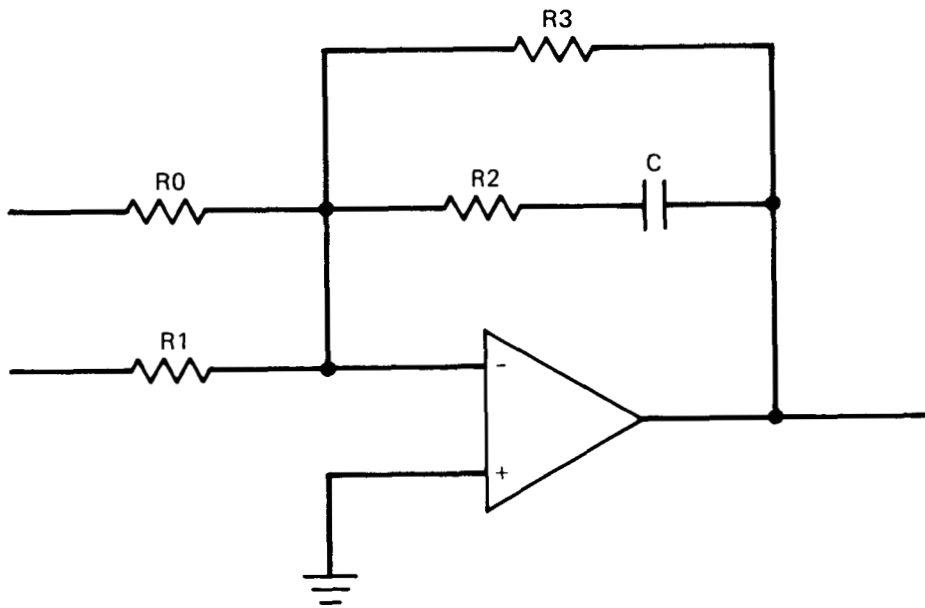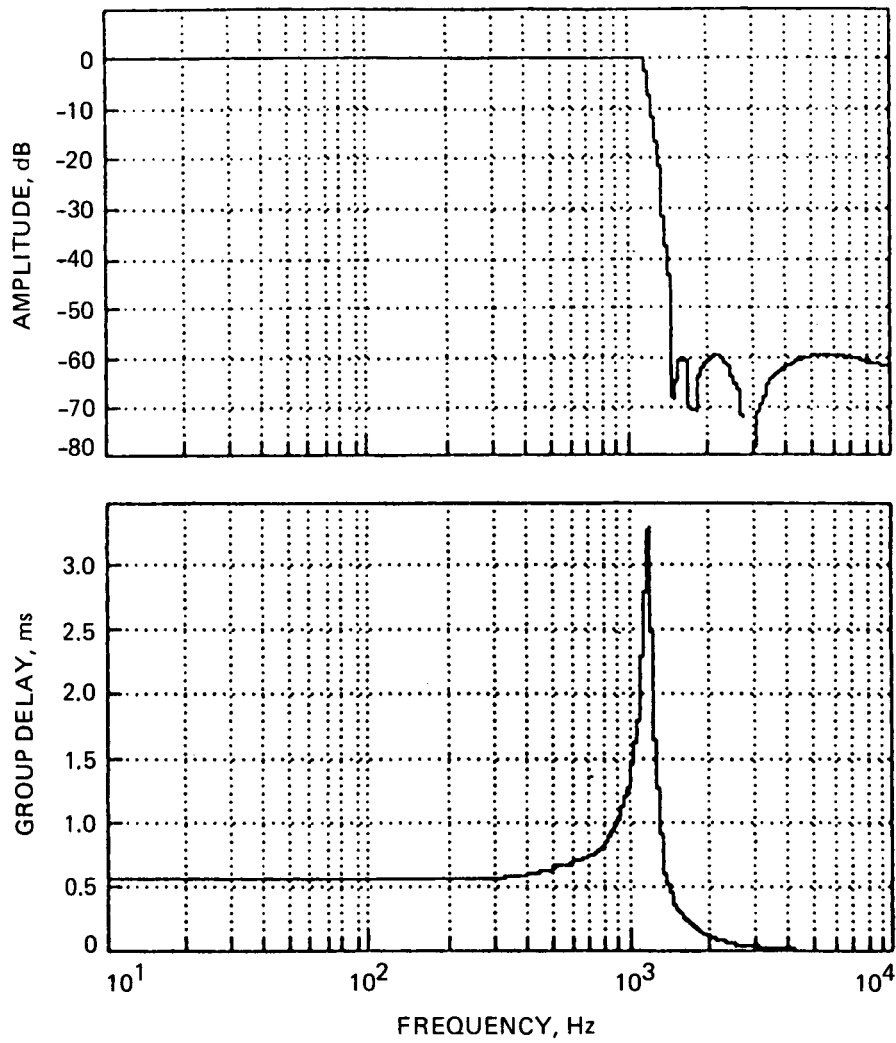

Figure A-4. Costas Loop Filter Structure

Filter Type: ELLIPTIC (Normalized to -3 dB Bandwidth)
Filter Order: 7
Cutoff Frequency: 1200 Hz

Figure A-5. Brick-Wall (Lowpass) Filter